



OPEN Co-application of polyethylene oxide (PEO), biochar, and seaweed fertilizer improves desert soil properties

Haoying Li¹, Huanan Liu^{1✉}, Bo Qi¹, Lianghao Zhai¹, Jiashun Ding¹ & Dan Qiu²

Improving water retention, erosion resistance and nutrients in desert areas is essential for ecological sustainability. This study evaluated the effects of biochar, polyethylene oxide (PEO), and seaweed fertilizer on the properties of desert sandy soil, focusing on water retention, erosion resistance, and soil nutrients. The sandy soil used in the study was taken from the Tengger Desert in Gansu, China, and an orthogonal experimental design was used to select three different proportions of biochar, PEO, and seaweed fertilizer. Compared with the control, applying of these three substances decreased bulk density by 5.8–9.6%, increased porosity by 8.3–14%, and increased water-holding capacity by 2.2–6.7%. The erosion rate decreased by more than 99%, and water-stable aggregates increased by 9.7–37.4%. Soil nutrients showed varying degrees of increase, and seed germination increased by 26.7%. The results of the principal component analysis showed that B6P0.6S2 had the best overall improvement effect. Therefore, a ratio of 6% biochar, 0.6% PEO, and 2% seaweed fertilizer is recommended to improve the properties of sandy desert soils. Overall, biochar, PEO, and seaweed fertilizer can improve the physical properties of desert sandy soil, enhance soil nutrients, and create a stable and suitable environment for plant growth.

Keywords Desert soil, Water retention capacity, Erosion resistance, Soil aggregate stability, Soil nutrients, Ecological restoration

Desertification is an environmental problem that seriously affects global ecosystems, climate, agricultural production, and human development^{1–3}. Desert soils usually have a low clay content and consist mainly of a large amount of sand and a small amount of silt^{4,5}. As the degree of desertification increases, the bulk density of the soil increases, and the soil water content, organic matter, and other components decrease^{6–9}. In addition, the weak water retention of desert soils makes it difficult for them to effectively meet the water requirements for plant growth, thus limiting the recovery of vegetation and the ecological construction process in desert areas¹⁰. Therefore, the key to combating desertification lies in improving the properties of desert soils and enhancing their water retention and nutrients. In recent years, soil improvement technology has received more and more attention in improving soil properties^{11,12}.

Biochar is a black material with rich pore space and specific surface area, and pyrolysis temperature and aging of biochar affect the potential merits of carbon source addition to desert soils¹³. The soil improvement effect of biochar has been reported to originate from the nature of the biochar itself, including the raw material, pyrolysis temperature, and particle size^{14,15}. The water-holding capacity of the biochar itself influences the water-holding capacity of the soil^{16,17}. Studies have shown that alkaline biochar produced at high temperatures can improve water-holding capacity and crop growth in sandy soils while increasing soil organic matter and plant nutrient content^{18,19}. Smaller particle sizes (< 5 mm) of biochar were the most effective in amending the soil^{20,21}. In addition, soil type also affects the effectiveness of biochar²². It has been studied that biochar has a significant amelioration effect in sandy soils²³. The application of biochar can improve the agglomerate stability, water retention capacity, and crop yield of degraded sandy soil, effectively improve the soil structure, increase the number and stability of agglomerates, and thus enhance the resistance to wind erosion^{24,25}. In addition, biochar can improve the water-holding capacity and soil nutrients of sandy soil, enhance the plant root system and aboveground biomass, and promote crop yield²⁶. All of the above studies have demonstrated the superior

¹School of Prospecting and Surveying, Changchun Institute of Technology, No. 3066 Tongzhi Street, Changchun 130021, Jilin, China. ²School of Emergency and Management, Changchun Institute of Technology, No. 3066 Tongzhi Street, Changchun 130021, Jilin, China. ✉email: liuhuanan@ccit.edu.cn

performance of biochar in soil improvement. However, it is worth noting that biochar can change the pH and porosity of soil through its dissolution in a short period, but the change of soil structure requires the interaction of biochar with plant roots and soil, which is a slow process²⁷.

In addition, polymers that can protect the soil from erosion damage in a short time are becoming increasingly popular²⁸. Some studies have found that PEO (polyethylene oxide) has significant advantages over substances such as PAM (polyacrylamide), CMC (carboxymethyl cellulose sodium), and PVA (polyvinyl alcohol). First, PEO has a high molecular weight, low biotoxicity, and is environmentally friendly²⁹. Second, the flocculation properties of PEO are not affected by pH and show better stability. In addition, the study found that PEO has a higher affinity for silica³⁰, whereas PAM needs to be in soils with a certain clay content to show effectiveness^{31,32}. To summarize, PEO is more suitable for soil improvement in desert soil areas with very low clay content.

Fertilizers extracted from seaweeds have significant biodegradable properties compared to conventional fertilizers. This property, coupled with its slower decomposition rate, effectively reduces the potential risk of over-application of fertilizers, thus achieving ecologically friendly use and conservation³³. Studies have shown that the addition of seaweed fertilizer improves the drought tolerance of tomato seedlings on sandy soils³⁴. Seaweed fertilizer also positively affects the growth and yield of wheat and improves the efficiency of farming on sandy soils³⁵. A field trial on sandy soils at the Ismailia Agricultural Company showed that the use of seaweed fertilizers was not only effective in increasing crop yields but also improved soil properties, reduced production costs, and reduced environmental pollution³⁶. Because of the above advantages, we chose seaweed fertilizer in this study to investigate its impact on nutrient supply and plant growth in desert soils and to provide a scientific basis for ecological restoration and sustainable agricultural development.

It has been studied that the combination of biochar and polymers can significantly improve the water-holding capacity of sandy soils, reduce soil water evaporation and infiltration rate, enhance the stability of aggregates, and promote crop growth³⁷. In addition, the pairing of biochar with organic fertilizers plays an important role in promoting C-N-P-S cycling in soil and increasing the number of associated microorganisms³⁸. The combination of biochar and fertilizer not only enhances plant nutrient uptake but also influences soil nutrient uptake and carbon dynamics by regulating carbon cycle enzyme activities and soil microbial communities^{39–41}.

Although some studies have highlighted the key role of biochar, fertilizer, and organic polymers in enhancing soil properties, relying on biochar and fertilizer alone without the application of organic polymers in desert areas may result in damage due to wind erosion before the soil structure is improved and the desired soil improvement objectives are not achieved. At the same time, if we only rely on biochar and polymers to improve desert soils, although polymers can form a solidified layer so that the soil will not be eroded in the short term, the solidified layer will gradually degrade over time, and due to the lack of organic matter and clay inside the soil, it will not be able to form stable aggregates, and will still be subjected to wind erosion in the end. In summary, soil improvement in desert areas requires comprehensive consideration of several factors.

Therefore, combining biochar, organic fertilizers, and polymers may be a good way to maintain the long-term productivity of sandy soils and alleviate the effects of drought erosion. Related studies have also confirmed the effectiveness of biochar-organic polymer-fertilizer combinations for sandy soil improvement and crop growth^{42–44}. However, there are relatively few indicators available for evaluating the effects of biochar, organic polymers, and fertilizer combinations on sandy soil properties, which makes it difficult to comprehensively assess the improvement in the overall quality of the soil. Also, there is a lack of clarity regarding the specific boundaries of substance addition. Therefore, the main objectives of this study are: I. To research the influence of co-application of the three substances on water holding capacity, dynamic water content, wind erosion resistance, water stability of aggregates, and soil nutrients in desert soils. II. Assessing the impact of three substances on seed germination and growth. III. Explore the appropriate application rates of PEO, biochar, and seaweed fertilizer in desert soils by combining a number of evaluation indexes such as water-holding capacity, aggregate stability, and germination rate.

Materials and methods

Materials

The soil selected for the study comes from the Tengger Desert. (37° 30′–40° N, 102° 20′–106° E) in Gansu Province, China. The soil was sieved through a 2 mm sieve before the experiment to remove impurities such as gravel and grassroots. Subsequently, the particle size distribution was analyzed using an LS-9 laser particle sizer, as shown in Fig. 1a. According to the geotechnical test standards; it was determined that the wind-sand soil sample had a bulk density of 1.61 g/cm³ and a natural moisture content of 0.44%.

Biochar was straw charcoal, purchased from Lianyungang Surui Processing Plant. The carbonization condition was 500 °C for 3 h. The biochar was sieved through a 0.5 mm^{20,21} sieve before testing. The basic information of the biochar is: bulk density of 0.55 g/cm³, pH value of 9.8 and C content of 68.7%.

Polyethylene oxide (PEO) was purchased from Shandong Hongquan Chemical Technology Co. The PEO powder was diluted to 0.2 g/100 ml and then stirred with a stirrer at 8000 r/min to ensure dissolution to give a 0.2% solution. Mass fractions of 0.2%, 0.4%, and 0.6% were selected for the experiment in this study. These concentrations were selected based on the available literature and the predominant soils of arid regions^{45,46}. The infrared spectrum (FTIR) of PEO is shown in Fig. 1b.

Seaweed fertilizer purchased from Shandong Akang Co. Seaweed fertilizer content: effective live bacteria ≥ 500 million/g, organic matter ≥ 60%, KANO seaweed extract ≥ 2%, indole rhizobium ≥ 0.3%, shrimp and crab shell powder + fishmeal ≥ 25%, active calcium + silicon + crude protein ≥ 30%, Zn + B + Fe + Mn + Mg + chitin 5%, *Bacillus cereus*.

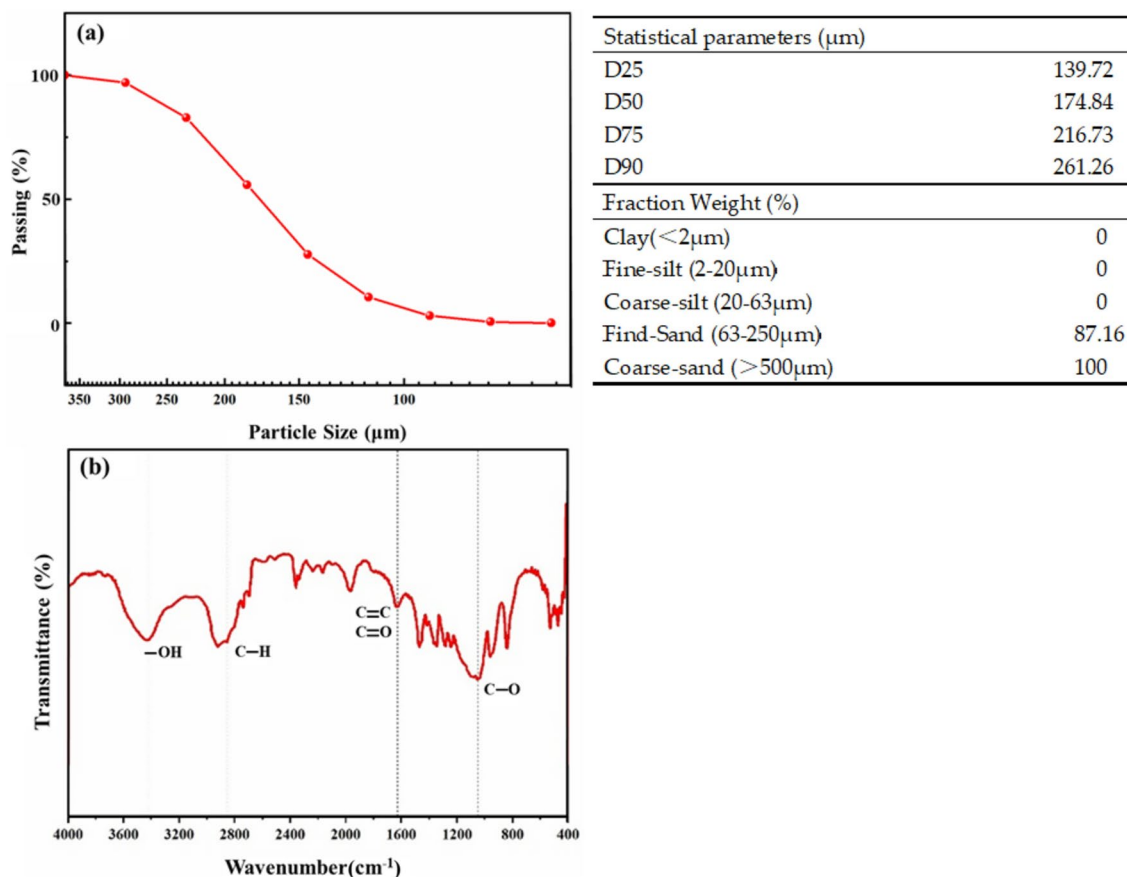


Fig. 1. (a) Soil particle size distribution. (b) FTIR of PEO solution.

Levels	Biochar (%)	PEO (%)	Seaweed fertilizer (%)
1	2	0.2	1
2	4	0.4	2
3	6	0.6	3

Table 1. Factor level table.

Experimental design

This study examines indoor experiments to find the best combination of three materials to improve desert soil properties.

An orthogonal array containing three levels of three factors (biochar, PEO, and seaweed fertilizer) was designed for the study. The factor level table is shown in Table 1, and the orthogonal design matrix is shown in Table 2.

Water retention test

The mixed 40 g of soil was placed in a container (50 mm diameter and 25 mm high) with a hole in the bottom and sprayed with PEO solution. The soil was then dried in an oven at 40 °C for 72 h to form a consolidated layer. Subsequently, it was placed in a container with pure water, and capillary action lifted the water to the upper part until the surface of the consolidated layer was wet. It was removed after 12 h of saturation, and it is worth noting that the petri dish was kept well hydrated during this process. Subsequently, the saturated samples were filtered until the last drop of water was extracted and quickly weighed. The wet samples were dried in an oven at 40 °C (Fig. 2a). The weight of the sand samples was determined, and the mass of water content calculated at 30 min intervals until the end when the weight was no longer changing and the mass water content was close to 0. Equation (1) shows the formula for *WHC* (water holding capacity).

$$WHC = (W_1 - W_0)/W_0, \quad (1)$$

where *WHC* is the water holding capacity, W_1 and W_0 are wet soil weight and dry soil weight, respectively.

Sample no.	Orthogonal design matrix		
	Biochar	PEO	Seaweed fertilizer
B0P0S0	0	0	0
B2P0.2S1	2%	0.2%	1%
B2P0.4S2	2%	0.4%	2%
B2P0.6S3	2%	0.6%	3%
B4P0.2S2	4%	0.2%	2%
B4P0.4S3	4%	0.4%	3%
B4P0.6S1	4%	0.6%	1%
B6P0.2S3	6%	0.2%	3%
B6P0.4S1	6%	0.4%	1%
B6P0.6S2	6%	0.6%	2%

Table 2. Table of orthogonal experiments for preliminary selection of formulation performance.

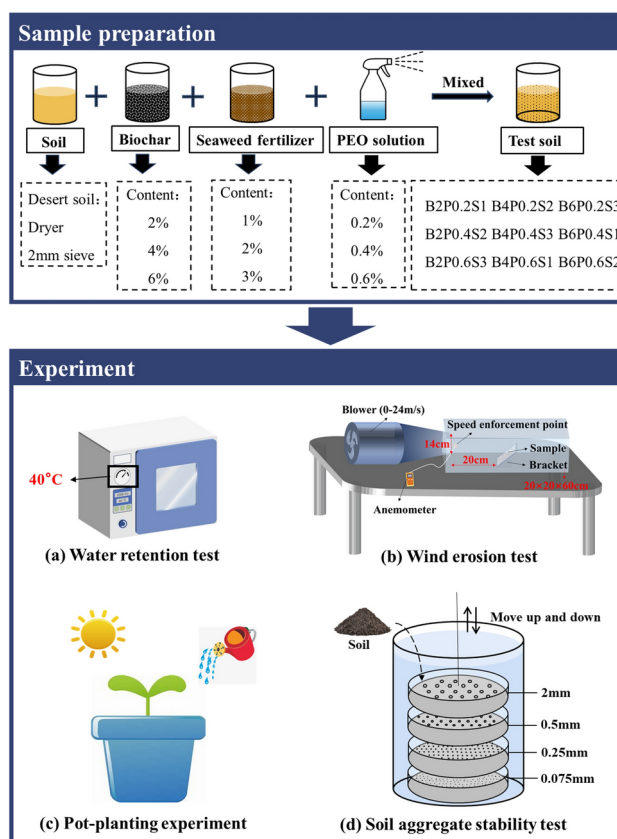


Fig. 2. Schematic diagram of the experimental process.

Wind erosion test

The study conducted wind erosion tests using a small homemade simple wind tunnel. A blower was used instead of a wind source, and the wind speed was adjustable between 0 and 24 m/s. The test section was a circular section with a diameter of 14 cm and a length of 60 cm. (Fig. 2b). Treated soils were filled into containers (160 × 120 × 40 mm), sprayed with PEO solution, and placed in a 40 °C drying oven for 72 h to form a consolidation layer. According to the China Meteorological Administration (CMA), wind speeds of 10–20 m/s are the main drivers of Tengger dust storms and severe dust storms⁴⁷. Therefore, a slope of 15° was chosen to simulate the windward side of the field dunes, and two wind speeds of 12 m/s and 18 m/s were designed. The total duration of each group was 40 min, 20 min for each wind speed. The sand was weighed before and after the test using an electronic scale to work out the erosion modulus of the sand (g/m²/min). After simulated wind

erosion, crusts were taken from three surface locations of the specimens, and the thickness was measured with a vernier caliper and averaged. Equation (2) shows the formula for the erosion rate.

$$R = (m_0 - m_1)/(S \times T), \quad (2)$$

where R is the wind erosion rate, $\text{g}\cdot\text{m}^{-2}\cdot\text{min}^{-1}$; m_0 is the mass of sandy soil before wind erosion, g ; m_1 is the mass of sandy soil after wind erosion, g ; S is the area of sand fixation specimen, m^2 ; T is the wind erosion time, min .

Soil aggregate stability index (wet sieving method)

Physical characteristics of the potting soil were analyzed after harvesting the plants after 50 days. 30.0 g of topsoil was placed on the top of a sieve with diameters of 2.0, 0.5, 0.25, and 0.075 mm, respectively, which were then submerged in water and manually moved up and down the sieve in the water approximately 3 cm 50 times over 2 min to separate the aggregate grades (Fig. 2d). Collecting, drying and weighing aggregates remaining on sieves of different sizes to obtain dry mass. In this study, the distribution of soil aggregates was characterized by assessing the mean weight diameter (MWD), geometric weight diameter (GMD), and the proportion of >0.25 mm aggregates ($W_{0.25}$). Equations (3), (4), (5) show the formulae for MWD , GMD , and $W_{0.25}$ respectively⁴⁸.

$$MWD = \sum_{i=1}^n x_i w_i, \quad (3)$$

$$GMD = \exp\left(\frac{\sum_{i=1}^n w_i \ln x_i}{\sum_{i=1}^n w_i}\right), \quad (4)$$

$$W_{0.25} = \frac{M_{0.25}}{M_t}. \quad (5)$$

x_i is the average diameter (mm) of the size class i , and w_i is the weight percentage (%) of aggregate in the size class i . M_t is the total mass (g) of the test soil, and $M_{0.25}$ is the mass of >0.25 mm agglomerates.

Pot-planting experiment

The indoor temperature was 20–25 °C, and relative humidity was 50–60% throughout the incubation period. Ten seeds were sown in free-draining pots (9 cm diameter and 11 cm high) and then covered with 0.5–1.0 cm of soil, followed by spraying PEO on the soil surface, and in the CK group, an equal quantity of water was applied (Fig. 2c). Germination was recorded until no further change by 12 h of light and 50 mL of water daily. Each treatment was replicated three times. Soil bulk density and porosity were determined using the ring knife method. After one month, 200 g of soil samples were collected for chemical analysis. Equation (6) is the formula for porosity determination.

$$T_p = 1 - \frac{p_b}{p_p} \times 100\%, \quad (6)$$

where T_p is total porosity, %; p_b is soil bulk density, g/cm^3 ; p_p is soil specific gravity (measured by specific gravity bottle method).

Soil alkali-hydrolyzed (AN), available phosphorus (AP) and potassium (AK) content by alkaline diffusion method⁴⁹ and combined extraction colorimetry with an ultraviolet spectrophotometer⁵⁰, respectively. Soil organic matter (SOM) was measured using the Walkley–Black method⁵¹.

Data analysis

Statistical analyses were performed using SPSS 25.0. One-way analysis of variance (ANOVA) was used for the data review. Tukey's HSD method of comparison was used for post hoc test. Before analyzing, all data were checked for normality, and their means and standard deviations were calculated. When the data did not fulfil the assumption of normal distribution, the rank sum test was used.

Integrated impact of different rates of treatment on soil was assessed by principal component analysis (PCA), and the best amelioration strategies were obtained by scoring and ranking.

Results

Water retention of soil

The results of the study showed that the WHC of the improved soil was significantly higher ($p < 0.05$) compared to B0P0S0. Figure 3 shows that the maximum WHC of the treatment groups B0P0S0, B2P0.2S1, B2P0.4S2, B2P0.6S3, B4P0.2S2, B4P0.4S3, B4P0.6S1, B6P0.2S3, B6P0.4S1, and B6P0.6S2 were 17.03, 17.26, 18.18, 18.84, 18.55, 20.8, 21.22, 21.71, 19.85 and 19.41% respectively. Compared with B0P0S0, the WHC of the improved

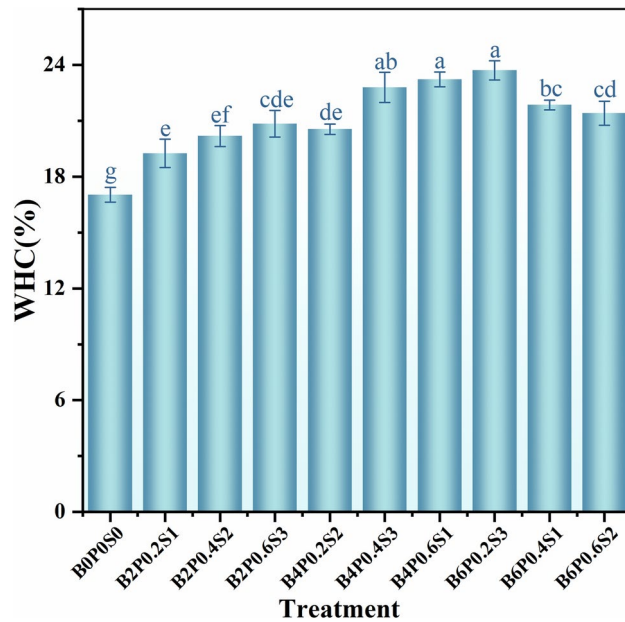


Fig. 3. Water-holding properties of treated desert soils.

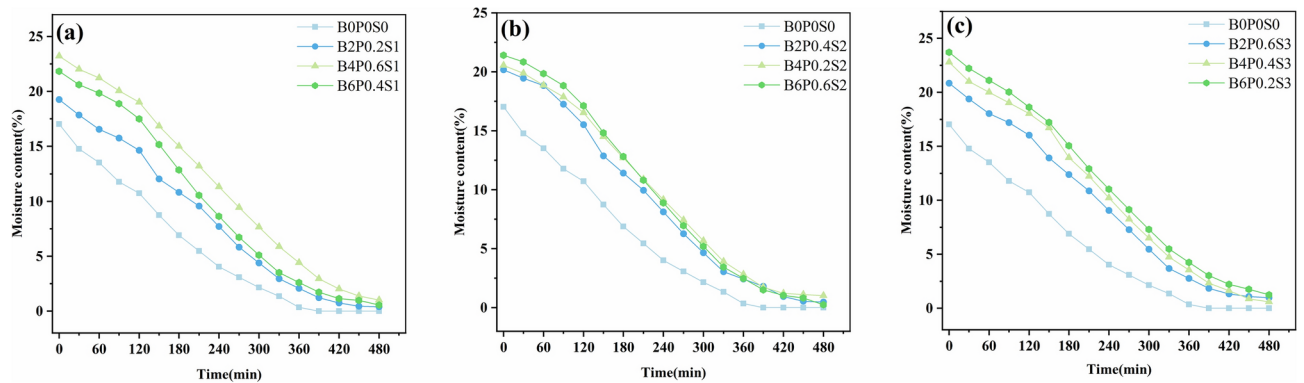


Fig. 4. Changes in water content of soil specimens as a function of time for 1% seaweed fertilizer treatment (a), 2% seaweed fertilizer treatment (b), and 3% seaweed fertilizer treatment (c).

soil in all treatment groups were increased. As can be seen in Fig. 11c, the pores of biochar improved the flow of air, water, and nutrients through the soil, while storing water and dissolved materials needed for microbial metabolism, which may be the main reason for the increase in soil water holding capacity.

Figure 4a–c show the moisture trends of soil samples at 1%, 2% and 3% of seaweed fertilizer content respectively. In these three graphs, we find that the dynamic water content of the groups tends to decrease with increasing evaporation time. However, compared with the control, the treated soil had a more robust water retention capacity under the drought experimental conditions. The dynamics of soil dynamic water content with evaporation time can be classified as a rapid decline and a steady decline. When the same mass of seaweed fertilizer was added to the soil, the soil samples with high biochar content sustained higher water content in the pre-drying period. However, after entering the stabilization period at 6 h of the test, soil samples with higher PEO content presented a more stable water content during the drying period than those with higher biochar content. After 8 h of drying test, the water content of the treated sample B6P0.6S2 still reached 1.56%. Even the worst water retention sample, B2P0.2S1, was able to stabilize its water content at 0.99%.

Wind erosion resistance of soils

The test results for wind erosion resistance are shown in Fig. 5a. Each of the treated soil samples showed excellent resistance to wind erosion compared to the control (B0P0S0). The control group experienced severe erosion damage at different wind speeds. Specifically, the erosion rate of each group increased with the increase of wind speed from 12 to 18 m/s. Among them, the erosion rate of the control group jumped from 165.3 to 825.1 g/m²/min, showing severe wind erosion. Although the B6P0.2S3 (Fig. 5c) treatment formed a thinner consolidation layer and the erosion rate increased when the wind speed increased from 12 to 18 m/s, it only increased from

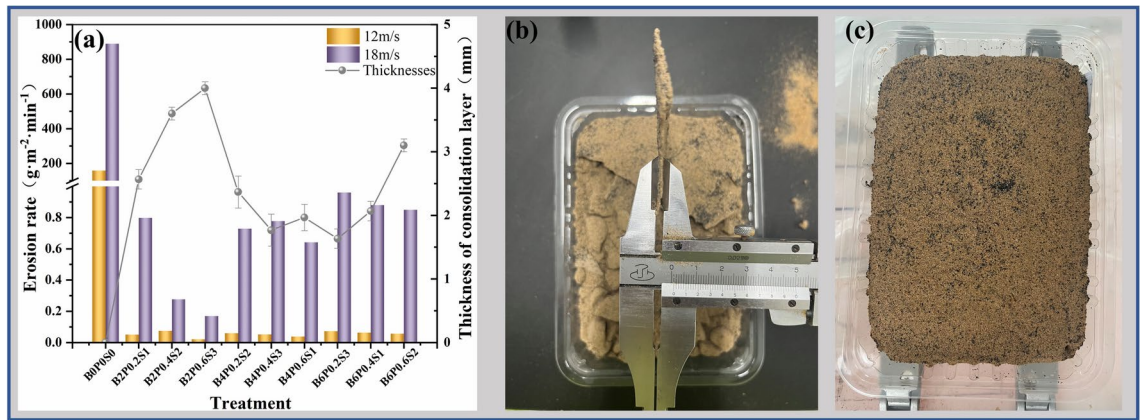


Fig. 5. (a) Erosion rates and crust thickness under different treatments. (b) Crust thickness measurements. (c) B6P0.2S3 Picture at the end of wind erosion.

0.381 to 0.602 g/m²/min. The erosion rate was almost negligible compared with the control, which indicated that the wind speed of sand initiation of the treated soils is all above 18 m/s. At the end of the wind erosion test, we also measured the thickness of the consolidation layer (Fig. 5b). The results showed that the thickness of the consolidation layer decreased with the addition of biochar and seaweed fertilizer when the PEO concentration was 0.2%. It is noteworthy, however, that the consolidation layer was not damaged by wind erosion in all treated soil samples except for the control.

Aggregate stability of soils

As shown in Fig. 6a, the water-stable soil aggregates were classified into 4 grain scale classes: >2 mm, 0.5–2.0 mm, 0.25–0.5 mm, and 0.075–0.25 mm. According to the data presented in Fig. 5a, the B0P0S0 treatment contributed 0 to >2 mm agglomerates, while the B6P0.6S2 treatment had the highest percentage of >2.0 mm agglomerates at 23.27%. The rate of 0.25–0.5 mm grain size aggregate was significantly ($p < 0.05$) enhanced by all treatments versus B0P0S0, with the B2P0.4S2 increasing from 4.43% in B0P0S0 to 15.9% in the proportion of 0.25–0.5 mm agglomerates. However, all nine groups of improved soils had significantly ($p < 0.05$) lower rates of 0.075–0.25 mm grain size aggregate than B0P0S0, especially under B6P0.6S2, where the rate of 0.075–0.25 mm grain size aggregate decreased from 89.13% in B0P0S0 to 55.2%.

Figure 6b–d demonstrates the results of $W_{0.25}$, MWD , and GMD for the assessment of agglomerate stability. The X, Y, and Z axes represent the different contents of PEO, biochar, and algal fertilizer, respectively. Based on the XY mapping, it can be seen that increasing PEO concentration and biochar content, $W_{0.25}$, MWD , and GMD showed an increasing trend. The highest values of 41.52%, 0.663 mm, and 0.61 were reached for these three indicators under the B6P0.6S2 treatment, respectively. This indicates a positive correlation between biochar and PEO in improving soil aggregate stability. Similarly, from the XZ mapping, it was found that $W_{0.25}$, MWD , and GMD increased with increasing content of seaweed fertilizer and PEO, and seaweed fertilizer and PEO also showed a positive correlation in improving soil aggregate stability. However, the results of YZ mapping showed that soil $W_{0.25}$, MWD , and GMD did not consistently increase with the increase of biochar and seaweed fertilizer content, but rather reached the highest value at a particular ratio, beyond which it may decrease, suggesting that the effects of biochar and seaweed fertilizer used in conjunction with each other on the stability of soil aggregates are positively correlated within a certain range, beyond which they may bring negative effects.

Plant germination and soil nutrients

Alfalfa was sown on treated soil to study the impact of PEO, biochar, and seaweed fertilizer on plant seed germination and growth. The pot test showed germination and growth results of alfalfa after 16 days of sowing, as shown in Fig. 7a,b. The results showed that alfalfa planted on treated soil germinated and grew well compared to the control (Fig. 7a). Figure 7b showed that the germination percentage of seeds grown in treated sandy soil was higher ($p < 0.05$) than that of seeds grown in natural sandy soil. The germination percentage of the B2P0.2S1 group was 33.33% higher than that of seeds grown in natural sandy soil. This was closely followed by B4P0.4S3 and B2P0.4S2 with an increase of 26.66 and 23.33, respectively, while the worst performer was B6P0.6S2 with only 56.67%, but still a rise of 10% relative to the control group. However, with the exact content of seaweed fertilizer, seed germination tended to decrease with the increase of biochar and PEO content.

As shown in Fig. 7c, biochar, PEO, and seaweed fertilizer increased ($p < 0.05$) soil nutrient indices compared to B0P0S0. The increase in seaweed fertilizer content showed a significant positive effect ($p < 0.05$) on soil alkali-hydrolyzed (AN), available phosphorus (AP), and potassium (AK) content. Soil AN and AP contents increased significantly ($p < 0.05$) from 32.03 and 1.20 in B0P0S0 to 108.67 g/kg and 14.93 g/kg in B4P0.4S3, respectively. Soil AK content increased from 201.79 g/kg in B0P0S0 to 246.43 g/kg under B6P0.2S3 treatment. Soil SOM increased with the increase of biochar. Significantly higher ($p < 0.05$) soil SOM was observed in B6P0.6S2 and

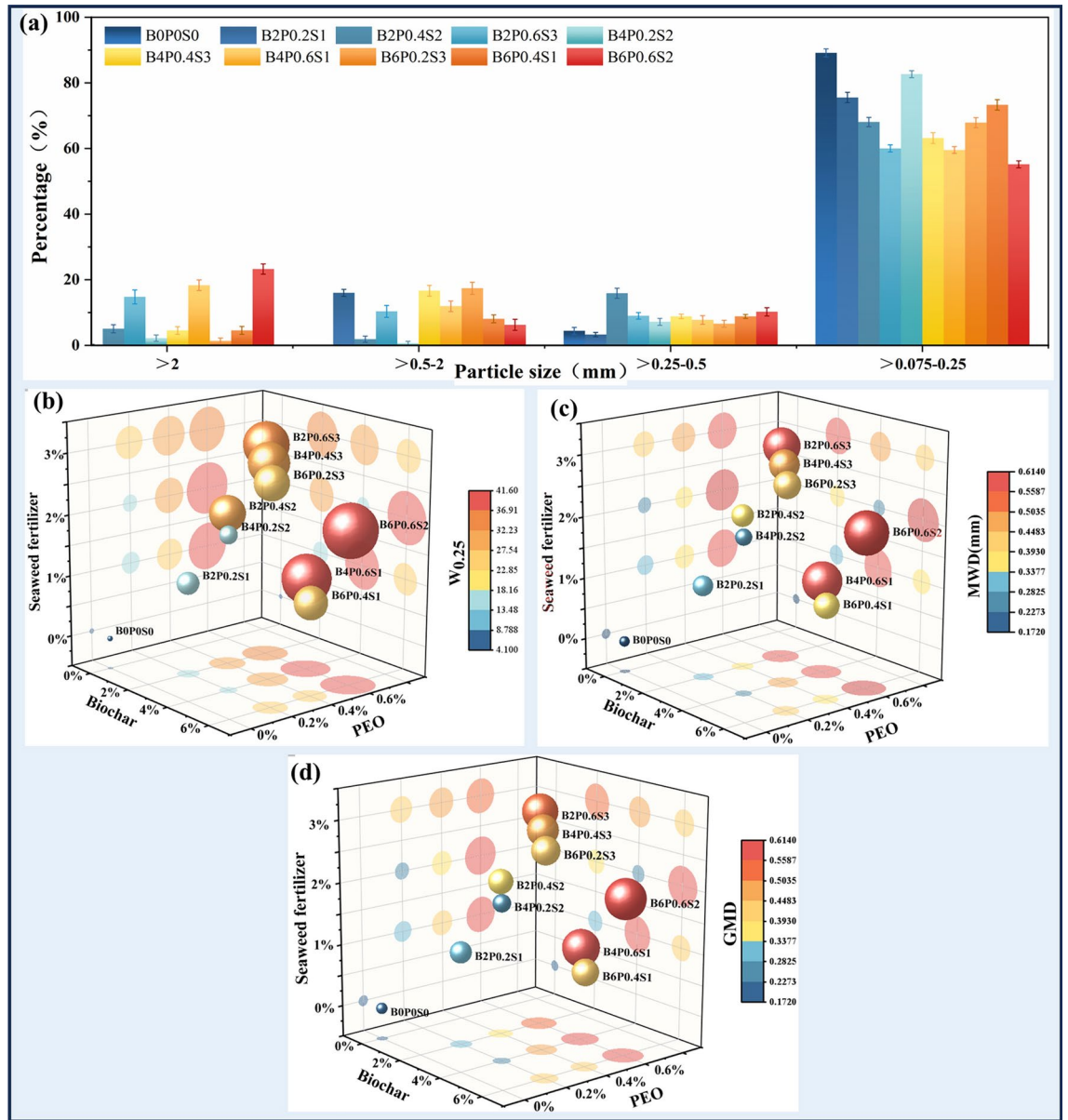


Fig. 6. Effect of different levels of biochar, PEO and seaweed fertilizer on grain diameter distribution (a), $W_{0.25}$ (b), MWD (c), GMD (d) of soil aggregates.

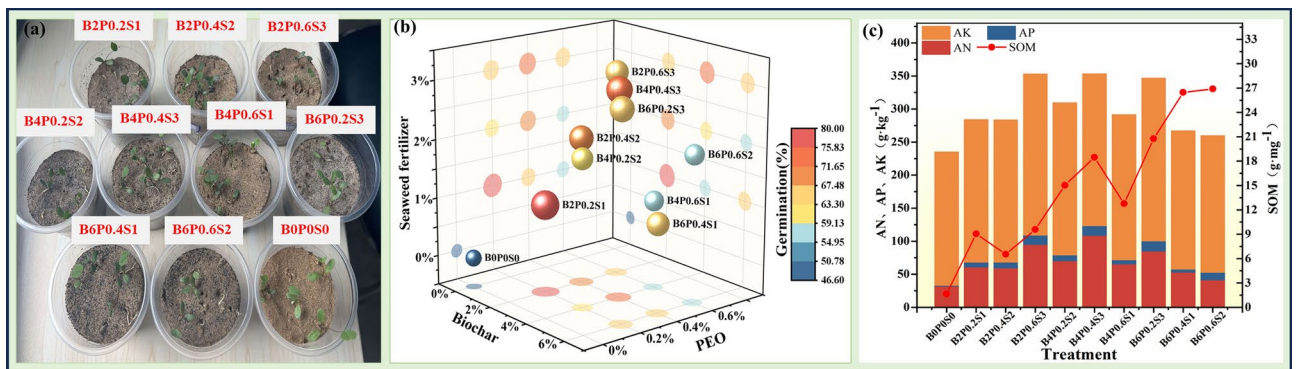


Fig. 7. Results of the potting experiment: (a) Plant growth, (b) seed germination, (c) soil nutrient content.

B6P0.4S1 compared to B0P0S0. In this case, the SOM of B6P0.6S2 increased from 1.65 to 26.9 g/mg followed by B6P0.4S1 which increased to 26.47 g/mg.

Changes in soil physical properties

The bulk density and porosity of the different treatments are shown in Fig. 8a. All treatments significantly increased the porosity and decreased bulk density compared to B0P0S0 ($p < 0.05$). With the same amount of biochar used, porosity gradually decreased with increasing PEO application, reaching a minimum value of 43.5% under the B6P0.6S2 treatment. In contrast, bulk density showed an increasing trend and reached a maximum value of 1.49 g/cm^3 under B4P0.6S1. When the amount of biochar was increased from B0 to B6, the bulk density increased from 40.06 to 44.23%, while the bulk weight decreased from 1.61 to 1.46 g/cm^3 . This indicated that the additions of biochar, PEO, and seaweed fertilizers lowered the bulk density of the soils to a certain extent while increasing the soil porosity.

Figure 8b demonstrates the grain size distribution of the soil samples after treatments with different material proportions of allotment. The results showed that the soil grain size of each treatment group was mainly dominated by fine-sand, followed by medium-sand, while the content of coarse-sand was low (the largest content of coarse-sand was 8.89% for B4P0.2S2, and the smallest content of coarse-sand was 4.32% for B2P0.2S1). The content of fine-sand decreased due to the addition of three substances. B2P0.4S2 (45.66%) and B4P0.4S3 (41.78%) decreased by 42.83% and 45.38% compared to B0P0S0 (87.16%), respectively. Whereas, the content of medium-sand increased. B2P0.2S1 (44.33%) and B6P0.4S1 (39.62%) increased by 33.66% and 28.95% respectively compared to B0P0S0 (10.67%). Although no clay was produced in the treatment groups, the silt content of the soil increased with the addition of the three substances. B2P0.2S1 showed the smallest increase of 3.81%, and B4P0.2S2 showed the largest increase of 6.62%

Integrated performance evaluation of biochar, PEO, and seaweed fertilizer co-application

The objective of this study was to comprehensively evaluate the improvement of desert physical properties by different treatments. A system of integrated soil quality assessment indicators was established using the principal component analysis (PCA). Eleven indicators, including soil saturated water holding capacity (*WHC*), bulk density (BD), porosity (T_p), proportion of water-stable aggregates ($W_{0.25}$), soil mean weight diameter (*MWD*), geometric mean diameter (*GMD*), alkali-hydrolyzed (AN), available phosphorus (AP), potassium (AK), organic matter (SOM), and germination rate (GER), were selected for comprehensive ranking.

The matrix of correlation coefficients for the eleven indicators is shown in Fig. 9. Overall, there were significant correlations between all indicators ($p < 0.05$). Among them, significant positive correlations were observed between *WHC* and *MWD*, *GMD*, $W_{0.25}$, AN, AP, AK, and SOM. Significant negative correlations were observed between BD and T_p ($p < 0.05$). The presence of significant correlations between $W_{0.25}$, *MWD*, *GMD*, and *WHC* suggests that changes in soil water holding capacity are closely related to soil aggregate stability. Similarly, significant correlations between BD, T_p , *MWD*, *GMD*, $W_{0.25}$, AN, AP, AK, SOM, and germination indicated that plant germination was closely related to improvement in soil physical properties as well as an increase in nutrients.

The contribution rates of different proportions of biochar, PEO, and seaweed fertilizer treatments were calculated by applying PCA. Simplify the above eleven indexes into F1 and F2 and calculate the composite score according to $F = 0.5266F1 + 0.2093F2$. Table 3 shows that the highest comprehensive ranking was obtained for B6P0.6S2, followed by B4P0.6S1 and B2P0.6S3.

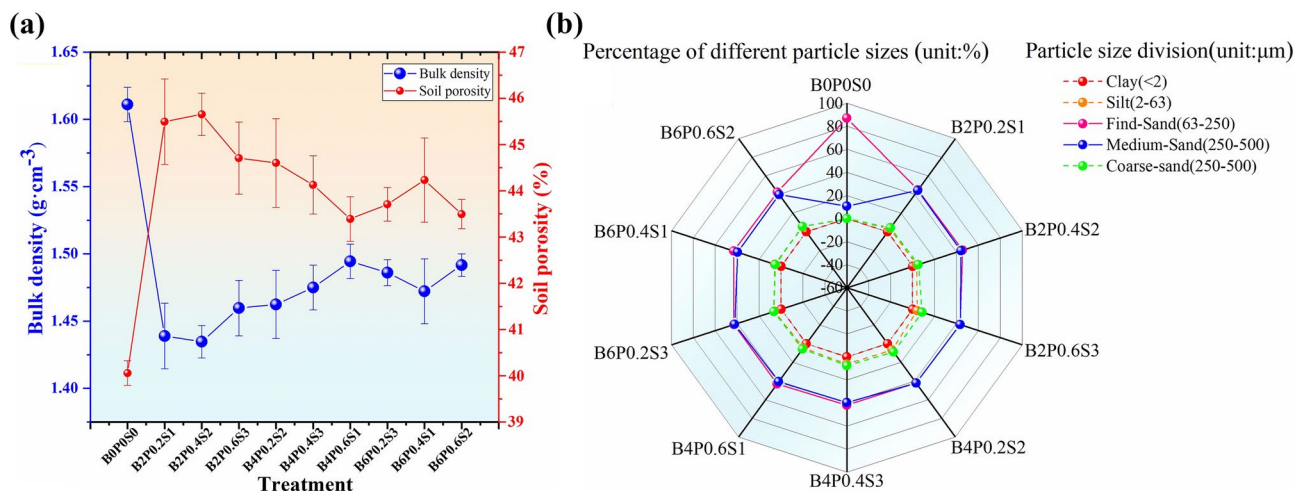


Fig. 8. Effect of different treatments on soil (a) bulk density and porosity, (b) particle size distribution.

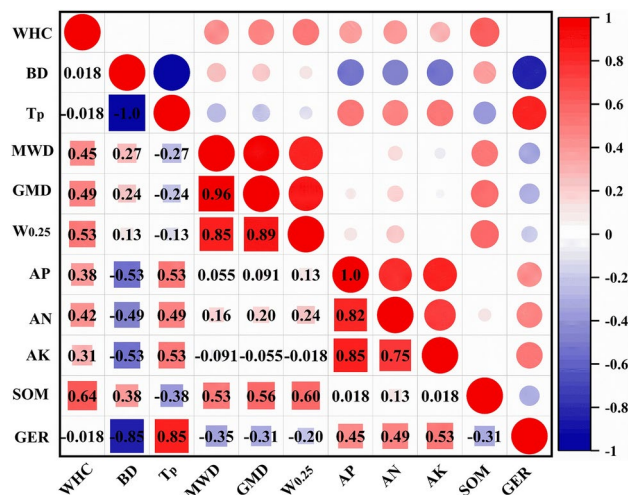


Fig. 9. Correlation heat map for 11 indices of soil.

Treatment	F1	F2	F	Ranking
B0P0S0	-1.56741	-2.23041	-129.227	10
B2P0.2S1	-1.16185	0.812687	-44.1667	9
B2P0.4S2	-0.65055	0.761027	-18.3267	7
B2P0.6S3	0.575503	0.650887	43.93	3
B4P0.2S2	-0.86461	0.636077	-32.2133	8
B4P0.4S3	0.48632	0.709243	40.45333	4
B4P0.6S1	1.15764	-0.68958	46.52333	2
B6P0.2S3	0.38124	0.56816	31.96667	5
B6P0.4S1	0.11681	-0.30298	-0.19	6
B6P0.6S2	1.52691	-0.91512	61.24667	1

Table 3. Orthogonal experimental design and optimal result.

Discussion

Mechanism of biochar, PEO, and seaweed fertilizer on soil water retention

Water is paramount for plant survival, especially in xeric desert areas, and water retention is a crucial focus of ecological restoration studies. In this study, the biochar increased the moisture holding properties of the soil, and this is the same as in former studies⁵². Because the large number of pores (Fig. 10b) and oxygen-containing functional groups (-OH and -COOH) on the surface of the biochar can bind with water molecules, increasing the retention of water^{53,54}. In this study, the particle size of the applied biochar was less than 0.5 mm, and the tiny biochar particles filled the macropores between the soils, increasing small pores and micropores in the soil mixture⁵⁵. The increase in porosity and specific surface area in the soil mixture provided more water storage pores and adsorption sites for water molecules, thus improving the water retention properties of the soil^{55,56}. At the same time, adding PEO also contributed significantly to the water retention of sandy soils. The presence of tiny pores in the membrane formed by the PEO solution (Fig. 10a) helps to reduce water flux and improve retention efficiency⁵⁷. But in practice, the PEO solution will cover the surface of the biochar to fill the structural pores (Fig. 10c), reducing the adsorption capacity of the pore structure of the biochar.

Mechanism of biochar, PEO, and seaweed fertilizer on soil resistance to wind erosion

In this study, PEO enhanced the wind erosion resistance of the soil, with specimens immobilized with only 0.2% PEO resisting wind speeds of 18 m/s without erosion damage. This was due to the presence of gaps between soil particles (Fig. 10d). The chemically cemented material fills the gaps (Fig. 10f) in the sand layer after the PEO solution is sprayed onto the soil surface. As the water evaporates, the material gradually solidifies into a solid, and the sand is tightly bonded to each other, forming a stable and uniform sand net (Fig. 11a), which effectively prevents wind dispersion⁵. As can be seen in Fig. 11b, the carboxyl functional bond in PEO, which improves the adsorption capacity of the polymer⁵⁸, links the loose sand grains into a whole through the macromolecular chain⁵⁹. Therefore, it is possible to form a solidified layer on the surface of the sand grains with a certain degree of resistance to wind erosion. In addition, biochar and seaweed fertilizer added to the soil as organic matter together improved soil agglomeration, increased the content of silt-clay and medium-sand particles,

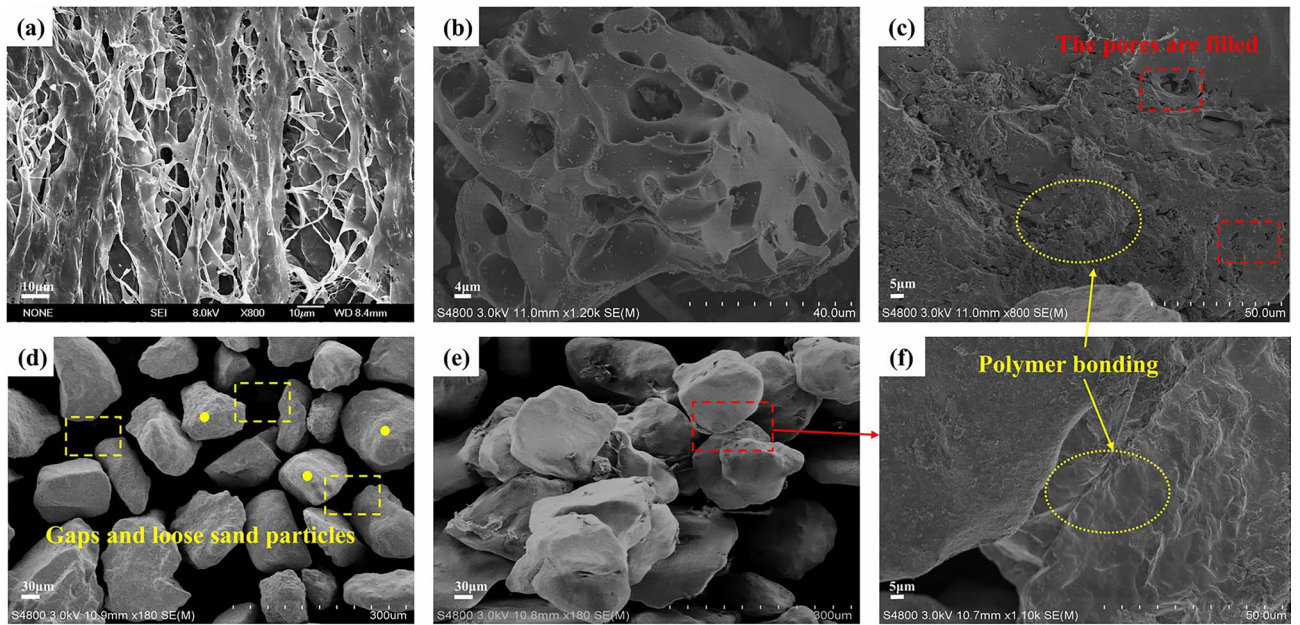


Fig. 10. (a) PEO membrane structure, (b) biochar pores, (c) PEO overlaying the biochar surface to fill the structural pores, (d) natural desert soil, (e) soil aggregates, (f) cementation between soil particles.

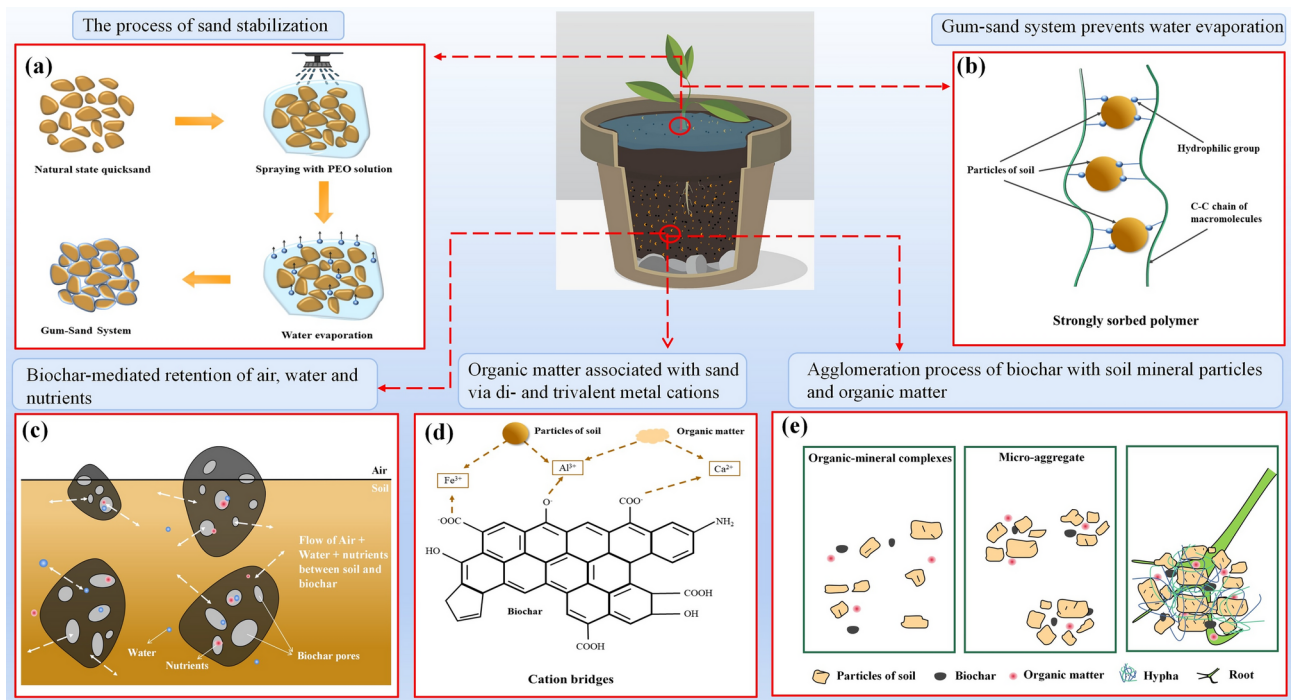


Fig. 11. Mechanism of amelioration of desert soil by co-application of biochar, PEO, and seaweed fertilizer.

and decreased the content of fine sand, thereby reducing wind erosion damage. This finding is consistent with previous studies^{5,24,60}.

Mechanisms of biochar, PEO, and seaweed fertilizer on soil aggregate stability

The content of $W_{0.25}$ increased to 15.9% (B2P0.4S2) after co-applying of biochar, PEO and algal fertilizer to the desert soil. The hydrophilic groups of the PEO solution cling onto the face of the soil grains (Fig. 11b), formed chemical bonds, and promoted the formation of agglomerates (Fig. 10e), which improved the binding capacity of the soil particles and dramatically increased aggregates in a brief time²⁸. Active functional groups

within the biochar interface form cationic bridges with soil particles (Fig. 11d). The cations act as a link between soil particles and organismic elements, contributing to the development of microaggregates and further incorporation into macroaggregates⁶¹. Clay and organic matter are key to soil agglomerate formation^{62,63}. The addition of the three substances elevated the silt–clay and organic matter content of the soil, which provided the organic bonding between soil particles for the formation of aggregates^{64,65}. In addition, where the biochar and soil particles come into contact with each other, soil microorganisms grow and multiply, producing large amounts of mycelium and slime⁶⁶, creating advantageous conditions for the formation of large agglomerates (Fig. 11e). Because the creation of large polymers in the soil mainly relies on the encapsulation of mycelium and plant roots in the soil⁶⁷. It can be inferred that planting plants can further encourage the development of large polymers, improve instability of desert soils, and prevent soil erosion.

Recommendations

In this study, biochar and seaweed fertilizer were selected as additives of exogenous organic matter, while PEO was used as a protective layer. PEO binds soil particles in a short period, while biochar and seaweed fertilizer enhance soil nutrients in a longer period, thus effectively counteracting the problems of evaporation of water, wind erosion, and loss of nutrients from desert soils, and providing an effective way of improving the environment of plant growth in sandy areas. Although these three substances can improve soil properties, it is not simply a matter of increasing the dosage to get the best results. One: the addition of all three substances increases production costs. Two: The dense film formed by high levels of PEO on the soil surface clogs soil pores and interferes with the transfer of air from the soil to the environment, thus affecting the availability of oxygen for vegetation roots and soil organisms. Third: High biochar and seaweed fertilizers can burn plant roots and damage plant growth.

In addition, this study determined the optimum treatment condition B6P0.6S2 by principal component analysis, in which the percentages of biochar, PEO, and seaweed fertilizer were 6%, 0.6%, and 2%, respectively. Moisturizing capacity, agglomeration stability, and nutrient content of the soil were significantly improved under this treatment. Although this study elucidated the mechanism of the combined application of these three substances for desert soil improvement, there are still limitations. For example, during the experimental operation, the PEO solution would cover the surface of the biochar and fill its pores, which reduced the adsorption capacity of the pore structure of the biochar as well as the cementing capacity between the PEO and the soil particles, leading to an unnecessary waste of resources. Therefore, there is a need for a more in-depth study on the optimal method of applying biochar, PEO, and seaweed fertilizer to the soil. In addition, the recommended optimal application patterns are based on small-scale laboratory experiments, and follow-up studies should be conducted with long-term field trials to more realistically assess the effects of these three substances in sandy desert soils.

Conclusions

Studies have shown that the combined application of biochar, PEO, and seaweed fertilizer can significantly improve the water retention capacity, erosion resistance, and soil nutrients of sandy desert soils, thus effectively promoting plant germination. The solidified layer formed by the drying of PEO can resist wind erosion and enhance water retention of soils under drought conditions. Biochar and seaweed fertilizer fill the gaps between soil sand particles, reduce soil bulk density, improve water-holding capacity and fertility, and provide more nutrients for plant growth. In addition, the combined application of these three substances improved the stability of soil aggregates in a short time, and increased the content of silt. In summary, the combined application of biochar, PEO, and seaweed fertilizer provides an effective soil improvement program for the sustainable development of agriculture in sandy areas.

Data availability

The datasets used and/or analyzed in this study are available upon reasonable request from the corresponding author (Huanan Liu; e-mail: liuhuanan@ccit.edu.cn).

Received: 28 September 2024; Accepted: 7 January 2025

Published online: 11 January 2025

References

1. Tao, W. Aeolian desertification and its control in Northern China. *Int. Soil Water Conserv. Res.* **2**, 34–41 (2014).
2. Verón, S. R., Paruelo, J. M. & Oesterheld, M. Assessing desertification. *J. Arid Environ.* **66**, 751–763 (2006).
3. Bestelmeyer, B. T. et al. Desertification, land use, and the transformation of global drylands. *Front. Ecol. Environ.* **13**(1), 28–36 (2015).
4. Zhou, Q. et al. First long-term detection of paleo-oceanic signature of dust aerosol at the southern marginal area of the Taklimakan Desert. *Sci. Rep.* **8**(1), 6779 (2018).
5. *Occurrence Regularity of Silt–Clay Minerals in Wind Eroded Deserts of Northwest China*. <https://www.mdpi.com/2071-1050/13/5/2998>.
6. Xie, Y. et al. Spatial heterogeneity of soil and vegetation characteristics and soil-vegetation relationships along an ecotone in Southern Mu Us Sandy Land. *China. J. Soils Sedim.* **15**, 1584. <https://doi.org/10.1007/s11368-015-1114-6> (2015).
7. Peng, F. et al. Changes of soil properties regulate the soil organic carbon loss with grassland degradation on the Qinghai-Tibet Plateau. *Ecol. Indic.* **93**, 572–580 (2018).
8. Zhou, H. et al. Network analysis reveals the strengthening of microbial interaction in biological soil crust development in the Mu Us Sandy Land, northwestern China. *Soil Biol. Biochem.* **144**, 107782 (2020).
9. Li, D. et al. Heterogeneity and loss of soil nutrient elements under aeolian processes in the Otindag Desert, China. *Aeolian Res.* **30**, 48–53 (2018).

10. *Influence of Biochar Application on Sandy Soil Hydraulic Properties and Nutrient Retention*. <https://www.semanticscholar.org/paper/Influence-of-biochar-application-on-sandy-soil-and-Uzoma-Inoue/9ae5498266a3f3dcf0929b1481af034bc08143070>.
11. Li, Z. et al. Woody organic amendments for retaining soil water, improving soil properties and enhancing plant growth in desertified soils of Ningxia, China. *Geoderma* **310**, 143–152 (2018).
12. *Effect of Some Soil Conditioners on Water-Use Efficacy, Growth, and Yield of Date Palm Siwi Grown in Sandy Soil Under Different Irrigation Regimes to Mitigate Climate Change*. <https://www.mdpi.com/2071-1050/14/18/11421>.
13. *Addition of Biochar to a Sandy Desert Soil: Effect on Crop Growth, Water Retention and Selected Properties*. <https://www.mdpi.com/2073-4395/9/6/327>.
14. Atkinson, C. J., Fitzgerald, J. D. & Hipps, N. A. Potential mechanisms for achieving agricultural benefits from biochar application to temperate soils: a review. *Plant Soil*. **337**, 1. <https://doi.org/10.1007/s11104-010-0464-5> (2010).
15. Gundale, M. J. & DeLuca, T. H. Temperature and source material influence ecological attributes of ponderosa pine and Douglas-fir charcoal. *For. Ecol. Manag.* **231**, 86–93 (2006).
16. Mao, J., Zhang, K. & Chen, B. Linking hydrophobicity of biochar to the water repellency and water holding capacity of biochar-amended soil. *Environ. Pollut.* **253**, 779–789 (2019).
17. Adhikari, S., Mahmud, M. A. P., Nguyen, M. D. & Timms, W. Evaluating fundamental biochar properties in relation to water holding capacity. *Chemosphere* **328**, 138620 (2023).
18. *Using Agricultural Residue Biochar to Improve Soil Quality of Desert Soils*. <https://www.mdpi.com/2077-0472/6/1/10>.
19. Alghamdi, A. G., Alomran, A., Ibrahim, H. M., Alkhasha, A. & Majrashi, M. A. Spent coffee waste-derived biochar improves physical properties, water retention, and maize (*Zea mays* L.) growth in sandy soil. *Sci. Rep.* **14**(1), 19753 (2024).
20. Obia, A., Mulder, J., Martinsen, V., Cornelissen, G. & Børresen, T. In situ effects of biochar on aggregation, water retention and porosity in light-textured tropical soils. *Soil Tillage Res.* **155**, 35–44 (2016).
21. Fu, G. et al. The role of biochar particle size and application rate in promoting the hydraulic and physical properties of sandy desert soil. *CATENA* **207**, 105607 (2021).
22. Wang, T., Stewart, C. E., Sun, C., Wang, Y. & Zheng, J. Effects of biochar addition on evaporation in the five typical Loess Plateau soils. *CATENA* **162**, 29–39 (2018).
23. Abel, S. et al. Impact of biochar and hydrochar addition on water retention and water repellency of sandy soil. *Geoderma* **202–203**, 183–191 (2013).
24. Pajouhesh, M., Gharahi, N., Iranmanesh, M. & Cornelis, W. M. Effects of vegetation pattern and of biochar and powdery soil amendments on soil loss by wind in a semi-arid region. *Soil Use Manag.* **36**(4), 704–713. <https://doi.org/10.1111/sum.12630> (2020).
25. *Effect of Biochar on the Physical and Structural Properties of a Sandy Soil*. <https://www.sciencedirect.com/science/article/abs/pii/S0341816218305551>.
26. Laghari, M. et al. Effects of biochar application rate on sandy desert soil properties and sorghum growth. *CATENA* **135**, 313–320 (2015).
27. Joseph, S. et al. How biochar works, and when it doesn't: A review of mechanisms controlling soil and plant responses to biochar. *Gcb Bioenergy* **13**(11), 1731–1764 (2021).
28. *A State-of-the-Art Review of Organic Polymer Modifiers for Slope Eco-Engineering*. <https://www.mdpi.com/2073-4360/15/13/2878>.
29. Lapointe, M. & Barbeau, B. Understanding the roles and characterizing the intrinsic properties of synthetic vs natural polymers to improve clarification through interparticle Bridging: A review. *Sep. Purif. Technol.* **231**, 115893 (2020).
30. Rubio, J. & Kitchener, J. A. The mechanism of adsorption of poly(ethylene oxide) flocculant on silica. *J. Colloid Interface Sci.* **57**, 132–142 (1976).
31. Levy, G. J. & Miller, W. P. Polyacrylamide adsorption and aggregate stability. *Soil Tillage Res.* **51**, 121–128 (1999).
32. Mamedov, A. I., Beckmann, S., Huang, C. & Levy, G. J. Aggregate stability as affected by polyacrylamide molecular weight, soil texture, and water quality. *Soil Sci. Soc. Am. J.* <https://doi.org/10.2136/sssaj2007.0096> (2007).
33. *Influence of Seaweed Liquid Fertilizer on Growth and Biochemical Characteristics of Arachis hypogea L. Under Field Trial*. <https://www.semanticscholar.org/paper/Influence-of-Seaweed-Liquid-Fertilizer-on-Growth-of-Sridhar-Rengasamy/ca718487b78189961d60fa0beb9ccee001e5fc03>.
34. *Seaweed Fertilizer Improved Drought Tolerance of Tomato Seedlings in Sandy Soil*. https://www.researchgate.net/publication/371052022_Seaweed_fertilizer_improved_drought_tolerance_of_tomato_seedlings_in_sandy_soil.
35. Salim, B. B. M. Influence of biochar and seaweed extract applications on growth, yield and mineral composition of wheat (*Triticum aestivum* L.) under sandy soil conditions. *Ann. Agric. Sci.* **61**, 257–265 (2016).
36. *Studying the Efficacy of Some Organic Compounds as a Source of Potassium Fertilization and their Effect on the Wheat-Peanut Crop System in Sandy Soil*. <https://doi.org/10.9734/ajsspn/2024/v10i1243> (2024).
37. *Effects of Biochar and Synthetic Polymer on the Hydro-physical Properties of Sandy Soils*. <https://www.mdpi.com/2071-1050/10/12/4642>.
38. Hu, W. et al. Biochar and organic fertilizer applications enhance soil functional microbial abundance and agroecosystem multifunctionality. *Biochar* **6**, 1. <https://doi.org/10.1007/s42773-023-00296-w> (2024).
39. Abideen, Z., Koyro, H.-W., Huchzermeyer, B., Gul, B. & Khan, M. A. Impact of a biochar or a biochar-compost mixture on water relation, nutrient uptake and photosynthesis of Phragmites karka. *Pedosphere* **30**, 466–477 (2020).
40. Ibrahim, M. M. et al. Biochar interaction with chemical fertilizer regulates soil organic carbon mineralization and the abundance of key C-cycling-related bacteria in rhizosphere soil. *Eur. J. Soil Biol.* **106**, 103350 (2021).
41. Huang, R. et al. Structural changes of soil organic matter and the linkage to rhizosphere bacterial communities with biochar amendment in manure fertilized soils. *Sci. Total Environ.* **692**, 333–343 (2019).
42. Aboelsoud, H. & Ahmed, A. Effect of biochar, vermicompost and polymer on wheat and maize productivity in sandy soils under drought stress. *Environ. Biodivers. Soil Secur.* <https://doi.org/10.21608/jenvbs.2020.29442.1095> (2020).
43. Kang, M. W. et al. Enhancement of soil physical properties and soil water retention with biochar-based soil amendments. *Sci. Total Environ.* **836**, 155746 (2022).
44. *The Fusion Impact of Compost, Biochar, and Polymer on Sandy Soil Properties and Bean Productivity*. <https://www.mdpi.com/2073-4395/13/10/2544>.
45. Mohawesh, O. & Durner, W. Effects of bentonite, hydrogel and biochar amendments on soil hydraulic properties from saturation to oven dryness. *Pedosphere* **29**, 598–607 (2019).
46. El-Asmar, J., Jaafar, H., Bashour, I., Farran, M. T. & Saoud, I. P. Hydrogel banding improves plant growth, survival, and water use efficiency in two calcareous soils. *Clean Soil Air Water* **45**, 1700251 (2017).
47. Guan, Q. et al. Climatological analysis of dust storms in the area surrounding the Tengger Desert during 1960–2007. *Clim. Dyn.* **45**, 903–913. <https://doi.org/10.1007/s00382-014-2321-3> (2015).
48. Shao, F. et al. Synergistic effects of biochar and carboxymethyl cellulose sodium (CMC) applications on improving water retention and aggregate stability in desert soils. *J. Environ. Manag.* **331**, 117305 (2023).
49. *Biochar and Organic Fertilizer Applications Enhance Soil Functional Microbial Abundance and Agroecosystem Multifunctionality*. <https://doi.org/10.1007/s42773-023-00296-w>.
50. *Effects of Different Factors on Fly Ash-Based Functional Soil and Its Oat Grass Cultivation*. <https://doi.org/10.3389/fpls.2022.1048101/full>.

51. Nelson, D. W. & Sommers, L. E. Total carbon, organic carbon, and organic matter. In *Methods of Soil Analysis* 961–1010. <https://doi.org/10.2136/sssabookser5.3.c34> (Wiley, 1996).
52. *Effect of Water Quality and Date Palm Biochar on Evaporation and Specific Hydrological Characteristics of Sandy Soil*. <https://www.mdpi.com/2077-0472/10/7/300>.
53. *Biochar for Environmental Management*. <https://doi.org/10.4324/9780203762264/biochar-environmental-management-johannes-lehmann-stephen-joseph>.
54. de Figueredo, N. A., da Costa, L. M., Melo, L. C. A., Siebeneichler, E. A. & Tronto, J. Characterization of biochars from different sources and evaluation of release of nutrients and contaminants. *Rev. Ciênc. Agron.* **48**, 3–403 (2017).
55. Adhikari, S., Timms, W. & Mahmud, M. A. P. Optimising water holding capacity and hydrophobicity of biochar for soil amendment—A review. *Sci. Total Environ.* **851**, 158043 (2022).
56. Yang, C., Liu, J. & Lu, S. Pyrolysis temperature affects pore characteristics of rice straw and canola stalk biochars and biochar-amended soils. *Geoderma* **397**, 115097 (2021).
57. *Cellulose/PEO Blends with Enhanced Water Absorption and Retention Functionality*. <https://www.semanticscholar.org/paper/Cellulose-PEO-blends-with-enhanced-water-absorption-Asghar-Samad/c58c35d66777fe7f409d83415f504b69a267b748>.
58. Botha, L. et al. Flocculation of oil sands tailings by hyperbranched functionalized polyethylenes (HBPE). *Miner. Eng.* **108**, 71–82 (2017).
59. Zang, Y. X., Gong, W., Xie, H., Liu, B. L. & Chen, H. L. Chemical sand stabilization: A review of material, mechanism, and problems. *Environ. Technol. Rev.* **4**, 307. <https://doi.org/10.1080/21622515.2015.1105307> (2015).
60. Jien, S.-H. & Wang, C.-S. Effects of biochar on soil properties and erosion potential in a highly weathered soil. *CATENA* **110**, 225–233 (2013).
61. *Organic Matter and Water-Stable Aggregates in Soils*. <https://www.semanticscholar.org/paper/Organic-matter-and-water%E2%80%90stable-aggregates-in-soils-Tisdall-Oades/4b365de4963549b572861e79ce0f89200c07c00b>.
62. *Influence of Pecan Biochar on Physical Properties of a Norfolk Loamy Sand*. https://www.researchgate.net/publication/43290031_Influence_of_Pecan_Biochar_on_Physical_Properties_of_a_Norfolk_Loamy_Sand.
63. Klüpfel, L., Keiluweit, M., Kleber, M. & Sander, M. Redox properties of plant biomass-derived black carbon (biochar). *Environ. Sci. Technol.* **48**, 5601 (2014).
64. Bai, S. H. et al. Combined effects of biochar and fertilizer applications on yield: A review and meta-analysis. *Sci. Total Environ.* **808**, 152073 (2022).
65. Wang, H., Shao, D., Ji, B., Gu, W. & Yao, M. Biochar effects on soil properties, water movement and irrigation water use efficiency of cultivated land in Qinghai-Tibet Plateau. *Sci. Total Environ.* **829**, 154520 (2022).
66. Rabbi, S. M. F. et al. Microbial decomposition of organic matter and wetting-drying promotes aggregation in artificial soil but porosity increases only in wet-dry condition. *Geoderma* **447**, 116924 (2024).
67. Forster, S. M. Microbial aggregation of sand in an embryo dune system. *Soil Biol. Biochem.* **11**, 537–543 (1979).

Acknowledgements

This work was supported by the Jilin Science and Technology Program (20230203130SF) (No. YDZ-J202301ZYTS228), Jilin Education Program (JJKH20230722KJ), Jilin Natural Science Foundation of China. Young Elite Scientists Sponsorship Program by CAST Eighth CAST Project No.: 2022QNRC001.

Author contributions

Haoying Li: Formal analysis, Investigation, Methodology, Validation, Writing—original draft. Huanan Liu: Conceptualization, Formal analysis, Project administration, Resources, Supervision, Validation, Writing—review & editing. Bo Qi: Funding acquisition, Project administration, Resources, Supervision. Lianghao Zhai: Funding acquisition, Project administration, Resources, Supervision. Jiashun Ding: Project administration, Supervision. Dan Qiu: Funding acquisition, Project administration, Resources, Supervision.

Declarations

Competing interests

The authors declare no competing interests.

Additional information

Correspondence and requests for materials should be addressed to H.L.

Reprints and permissions information is available at www.nature.com/reprints.

Publisher's note Springer Nature remains neutral with regard to jurisdictional claims in published maps and institutional affiliations.

Open Access This article is licensed under a Creative Commons Attribution-NonCommercial-NoDerivatives 4.0 International License, which permits any non-commercial use, sharing, distribution and reproduction in any medium or format, as long as you give appropriate credit to the original author(s) and the source, provide a link to the Creative Commons licence, and indicate if you modified the licensed material. You do not have permission under this licence to share adapted material derived from this article or parts of it. The images or other third party material in this article are included in the article's Creative Commons licence, unless indicated otherwise in a credit line to the material. If material is not included in the article's Creative Commons licence and your intended use is not permitted by statutory regulation or exceeds the permitted use, you will need to obtain permission directly from the copyright holder. To view a copy of this licence, visit <http://creativecommons.org/licenses/by-nc-nd/4.0/>.

© The Author(s) 2025